A Wideband Power-Efficient Inductive Wireless Link for Implantable Microelectronic Devices Using Multiple Carriers

Suresh Atluri[1] and Maysam Ghovanloo[1,2]

[1]Department of Electrical and Computer Engineering, [2]Department of Biomedical Engineering,
North Carolina State University, Raleigh, NC, USA
mghovan@ncsu.edu

Abstract— **This paper presents a novel inductive link for wireless transmission of power and data to biomedical implantable microelectronic devices using multiple carrier frequencies. Achieving higher data bandwidth without compromising the power efficiency is the driving force to use two separate carriers. Two separate pairs of coils have been utilized for inductive power and forward data transmission. One major challenge, however, is to minimize the interference among these carriers especially on the implantable side, where size and power are highly limited. Planar power coils with spiral shape are optimized in geometry to provide maximum coupling coefficient, *k*. The data coils are designed rectangular in shape and wound across the power coils diameter to be oriented perpendicular to the power coil planes. The goal is to maximize data coils direct coupling, while minimize their cross-coupling with the power coils. The effects of coils geometry, relative distance, and misalignments on the coupling coefficients have been modeled and experimentally measured.**

I. Introduction

An inductive link between two magnetically-coupled coils is being used to wirelessly energize implantable micro-electronic devices (IMDs) with high power requirements such as neuromuscular stimulators, cochlear implants, and visual prostheses [1]-[3]. These IMDs are either battery-less and should be continuously powered from an external portable battery, or have miniature rechargeable batteries that should be inductively charged on a regular basis. In both cases, the inductive power transmission should be very efficient to minimize the size of the external battery, and eliminate overheating the surrounding tissue by thermal dissipation within the implant or within the tissue as a result of surpassing the exposure limit to electromagnetic field [4].

IMDs that substitute sensory functions also require sizeable amounts of real-time data to interface with a large number of neurons. The neural interface has been established by means of tens to hundreds of stimulating sites, depending on the application, which are driven through multiple parallel channels [5]. As a result, wideband data transmission is another requirement for the wireless link, which should also be robust enough not to be affected by patient's motion artifacts or minor coils misalignments.

The traditional single carrier inductive link designs [6]-[8] cannot simultaneously provide power efficiency, data bandwidth, and coupling insensitivity at the levels required by today's increasingly challenging neuroprosthetic applications. For example, increasing the carrier frequency can result in wider bandwidth for data transmission. However, it degrades power transmission efficiency due to more power deposition in the tissue and more dissipation in the external and internal power conditioning blocks.

We proposed in [9] utilizing three carrier signals at three different frequencies and amplitude levels which are proper for the specific functions of a wireless link (1) a low-frequency (f_P < 1 MHz) high-amplitude carrier for power transmission, (2) a medium-frequency (f_{FD} = 25 ~ 50 MHz) medium-amplitude carrier for forward data transmission, and (3) a high-frequency (f_{BT} > 1 GHz) low-amplitude carrier for back telemetry. Employing multiple carriers would help to effectively isolate many of the conflicting requirements in design of the wireless link. On the other hand, the main challenge in using multiple simultaneous carriers for data and power transmission is the interference.

We believe that the most difficult part of this problem is eliminating the strong power carrier interference with data carrier on the implantable receiver side, where the power budget and size are extremely limited. To address this issue, the following measures are adopted:

1- Two individual pairs of coils are dedicated to power and forward data transmission. The geometry and orientation of the coils are designed in order to occupy a small space, maximize direct coupling within each pair, and minimize the cross coupling between the pairs.

2- The data carrier is frequency shift keyed (FSK) [10], to be more robust against interference as opposed to amplitude shift keying (ASK), which is the method that is used in most similar applications [1]-[3].

3- The data carrier, f_D, is chosen 25 times higher than the power carrier, f_P, to provide enough spacing between the two carrier components in the frequency domain. This would allow reliable detection of the forward data bits with proper tuning, on-chip filtering, and utilization of a novel FSK demodulation technique [10].

Fig. 1 shows an IMD block diagram with two individual carriers for power and forward data transmission. L_1 and L_2 form the inductive power transmission pair, while L_3 and L_4 constitute the forward data link. The rest of this paper is dedicated to the geometrical considerations in design of this dual carrier inductive link [9] as well as simulation and measurement results with experimental prototype models.

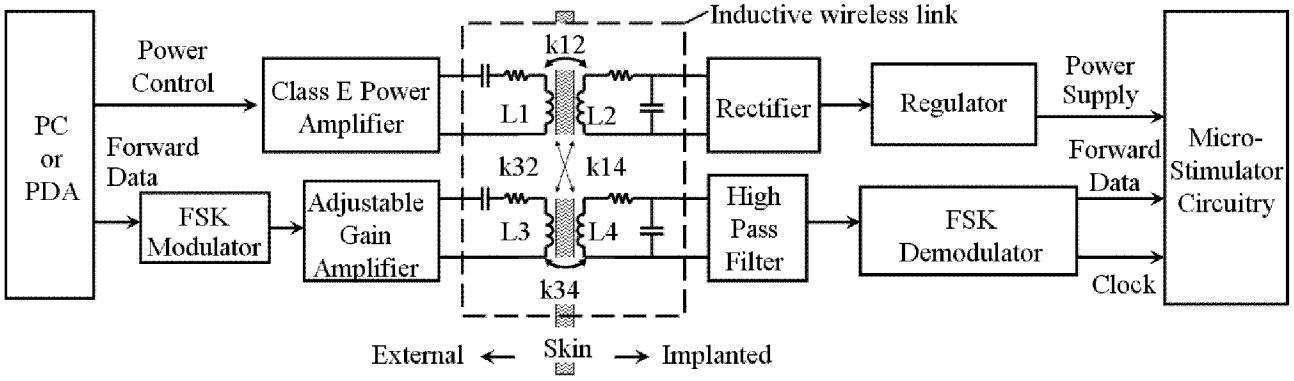

Figure1. Block diagram of an implantable microelectronic device for neural stimulation. The wideband power-efficient inductive wireless link, which is the focus of this paper, is enclosed in a dashed box [9].

II. Inductive Link Geometric Considerations

A. Power Coils

The inductive link power transmission efficiency, $\eta\%$, is the key parameter in design of the power coils, which should be maximized. Other important factors are the coils size, separation, and some surgical considerations. In a simplified scenario, $\eta\%$ is proportional to $Q_i Q_j k_{ij}^2$, where Q_i and Q_j are the quality factors of the external primary and internal secondary coils, respectively. k_{ij} is the coupling coefficient between the two coils [6]. Q_i and Q_j can be increased by reducing coils parasitic resistance and forming inductive-capacitive (LC) tank circuits, tuned at f_P. The most effective parameter, k_{ij} however, depends on the coils self and mutual inductance, L_i and M_{ij}, which in turn depend on their geometry, separation, and orientation.

$$k_{ij} = \frac{M_{ij}}{\sqrt{L_i \times L_j}} \tag{1}$$

We chose circular, planar, spiral geometry that is currently the most widely used in design of the inductively powered IMDs [2], [7], [9]. The spiral coils are fairly robust against lateral misalignments and their optimal design has been covered in the literature [7], [9].

B. Data Coils

The geometry and orientation of the data coil pair is significantly important since the power carrier amplitude is usually much larger than the data carrier amplitude on the transmitter side. Therefore, unless the interference between the power and data carriers is adequately reduced on both sides, demodulation and detection of the data bits would be impossible. Unfortunately none of the methods suggested in the literature [11] is quite functional. In the coaxial approach, there is the same flux linkage between the transmitter power coil and both receiver power and data coils. This would result in a strong cross coupling between the transmitter power and receiver data coils, which results in the saturation of the implant data receiver by the strong power carrier interference. In the orthogonal approach, if the data coils are wound around the power coil windings as suggested, similar to current transformers, then current variations in the power coils will induce electromotive force (EMF) across the data coils and cause significant power carrier interference with the data signal.

Our novel approach is first, to utilize the relationship between M_{ij} and the relative orientation of two coaxial conductive loops to minimize undesired mutual couplings.

$$M_{ij}(d_r, \theta) = M_{ij}(d_r, 0)\cos(\theta) \tag{2}$$

where d_r is the relative center to center distance between the loops, and θ is the angle between their planes. Second, we zero out the total current passing through the data coil loops. In our geometrical design of the data coils, shown in Fig. 2, the first requirement is achieved by placing the data coils in the same plane, perpendicular to the power coil planes ($\theta = 90°$). The second requirement is satisfied by winding the data coils across the entire diameter of the power coils to encompass equal numbers of wires passing current in two opposite directions, thus canceling out their interfering EMF. An additional advantage of this approach is elongating the parallel segments of the data coils, L_3 and L_3, thus increasing their coupling coefficient, k_{34}.

III. Modeling and Simulation Results

Closed form analytical solutions for calculating self and mutual coil inductances either become too complicated or lose their accuracy for multiple coils shown in Fig. 2 [7], [8]. In order to more accurately model coils with various geometries, one should either use tabulated parameterized equations [12], or coil analysis software. We have developed MATLAB code to model multiple coupled coils with arbitrary geometries by generating the coordinates of the coils for FastHenry-2 [13]. Using these models, we reported the parameters that have the most significant effects on maximizing direct coupling between the two power coils (k_{12}) or data coils (k_{34}), while minimizing the cross coupling between these pairs (k_{32} and k_{14}) [9].

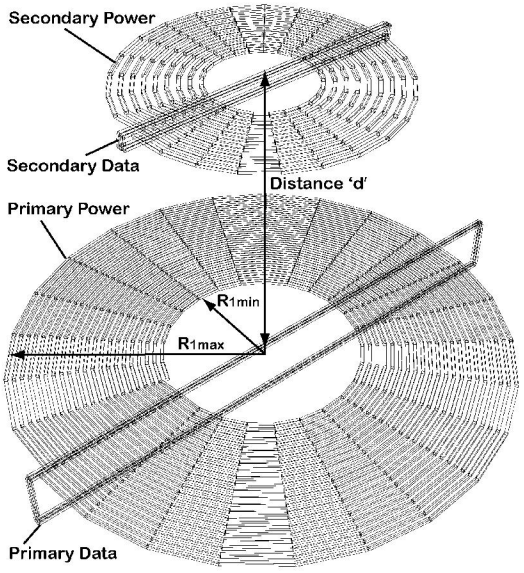

Figure 2. Three dimensional rendering of the data and power transmission coils in the new multi-carrier inductive link.

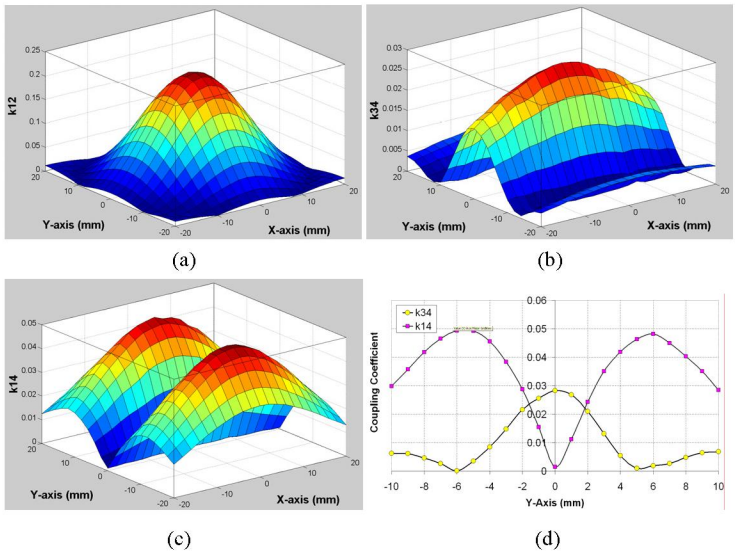

Figure 3. Direct and cross coupling coefficients vs. X and Y axis misalignments (a) k_{12} (b) k_{34} (c) k_{14} (d) Overlapping k_{34} and k_{14} at X = 0 mm to observe the range of acceptable misalignments along Y-axis.

Fig. 3 shows further simulation results on how k_{12}, k_{34}, and k_{14} change as a result of coils lateral misalignments at constant d_r = 10 mm. The spiral power coils show a high direct coupling when they are perfectly aligned. In Fig. 3a, k_{12} shows similar bell-shaped drops along X and Y axes misalignments due to the power coils symmetry. On the other hand, k_{34} and k_{14} in Figures 3b and 3c show that data coils are far less sensitive to misalignments along the X-axis (along their length ∅) compared to the Y-axis. It can be concluded from these simulations that Fig. 2 coil configuration can very well handle coil misalignment along X. However, along Y, the misalignments are acceptable as long as $k_{34} \geq k_{14}$. This can be seen more clearly by overlapping k_{14} and k_{34} surfaces in Fig. 3d. In order to reduce data coils sensitivity against Y misalignment, one possible solution is to add a second pair of forward data coils perpendicular to the first pair (L_3 and L_4).

IV. Measurement Results

Two sets of prototype data/power coil pairs similar to Fig. 2 were hand made for experimental measurements and comparison with simulation results. Table I summarizes the specifications of these coils. The coils were designed for the optimal relative distances, d_r, of about 10 mm and 18 mm for Set1 and Set2, respectively.

A network analyzer (Agilent E5071B) was used to perform two-port measurements on every pair of coils in the inductive link and obtain the S-parameters, while changing the relative distance between coils. The S-parameters were then converted to Z-parameters using Agilent Advanced Design System (ADS) software. The two-port Z matrix includes the self and mutual inductances, which can be extracted from (3) at each operating frequency, and substituted in (1) to calculate k_{ij}.

TABLE I
HANDMADE POWER AND DATA COILS SPECIFICATIONS

Parameters	Set1	Set2
L_1, N_1, R_{min1}, R_{max1}	6.4, 17, 6.5, 18	36, 34, 7, 32
L_2, N_2, R_{min2}, R_{max2}	1.88, 9, 6, 13	1.2, 10, 3, 11
L_3, N_3, W_3^*, $\varnothing_3^+$	0.41, 3, 7, 40	0.6, 3, 7, 64
L_4, N_4, W_4^*, $\varnothing_4^+$	0.31, 3, 7, 30	0.25, 3, 7, 26
Wire Gauge #, ∅	22, 0.6425	22, 0.6425

All inductances are in µH.
All sizes are in mm.
* Width of the rectangular data coil
+ Length of the rectangular data coil

$$Z_{ij} = \begin{bmatrix} R_i + jwL_i & R_{ij} - jwM_{ij} \\ R_{ji} - jwM_{ji} & R_j + jwL_j \end{bmatrix} \quad (3)$$

The measured and simulated (from FastHenry-2) values of k_{ij} for direct and cross couplings between power and data coils are shown in Fig 4, while d_r is changed from 10 to 30 mm. It can be seen that there is a good agreement between simulated and measured values of k_{12} and k_{34}. Coupling between the power coils is pretty strong at d_r = 10 mm. Even though we have not optimized L_1 and L_2 for maximum power efficiency, it can be concluded from [14] that with k_{12} = 0.228 for Set1, $\eta\% > 60\%$ can be achieved. Also as expected, there is a sharper drop in k_{12} for smaller transmitter coil (Set1) than the larger one (Set2).

Fig. 3c shows that in order to achieve minimum cross coupling, all coils should be symmetrical and axially aligned. However, reaching close symmetries in handmade coils is very difficult. Therefore, we adjusted the height of the receiver coil to find the Y-axis misalignment at which k_{14} was minimal. Fig. 4c shows k_{14} vs. vertical misalignment for Set2 with minimum achieved at Y = 2.6 mm, which follows the same trend as Fig. 3c. With these

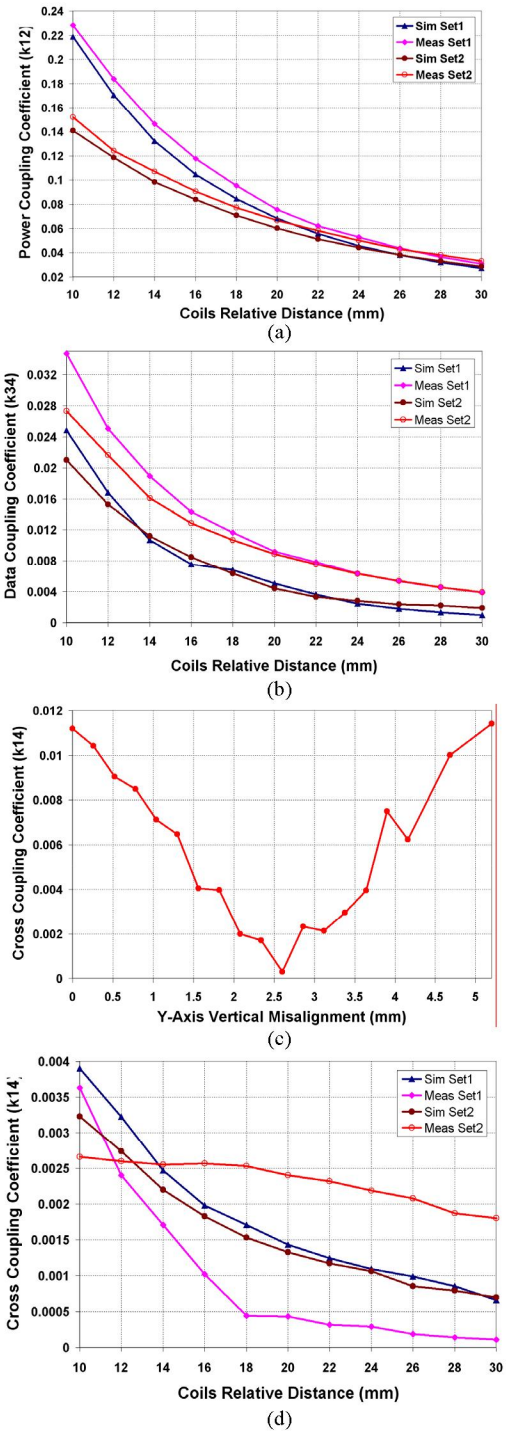

Figure 4. Measured and simulated values of coupling coefficient between (a) Power coils, k_{12} and (b) Data coils, k_{34}. (c) Y-axis misalignment between coils to find minimum cross coupling for Set2 (d) Measured and simulated values of cross coupling coefficient, k_{14}, between transmitter power coil, L_1, and receiver data coil, L_4.

adjusted heights, Fig. 4d compares simulated and measured k_{14} values for both sets. Fabrication inaccuracies and the fact that k_{14} is very small have resulted in some discrepancies between simulated and measured values. Nevertheless, results are in the same range.

The main point to be made here is that with the novel multi-carrier inductive link configuration presented in this paper, the undesired cross coupling, k_{14}, in Fig. 4d is at least one order of magnitude smaller than the desired direct coupling, k_{34}, in Fig. 4b. This can significantly help in reducing power carrier interference with the received data signal on the implant side, especially when combined with frequency separation and high pass filtering.

V. Conclusions

A new approach for wireless efficient power and wideband data transmission to implantable microelectronic devices is presented using individual carriers at different frequencies and amplitude levels through separate coil pairs. Novel coil geometries and orientations have been proposed for the inductive link to increase direct coupling between power and data coil pairs, while decreasing cross coupling between the pairs to reduce interference between carriers. Simulation and modeling results using coil analysis software and measurement results using handmade coils and a network analyzer indicate the functionality of this approach.

References

[1] B. Smith *et al.*, "An externally powered, multichannel, implantable stimulator-telemeter for control of paralyzed muscle," *IEEE Trans. Biomed. Eng.*, no. 4, pp. 463-475, Apr. 1998.

[2] Advanced Bionics, HiRes™ 90K Bionic Ear Implant, Available: http://www.bionicear.com/products/90k_implant.asp

[3] G.J. Suaning and N.H. Lovell, "CMOS neuro-stimulation ASIC with 100 channels, scalable output, and bidirectional radio-freq. telemetry", *IEEE Trans. Biomed. Eng.*, vol. 48, pp. 248-260, Feb. 2001.

[4] IEEE standard for safety levels with respect to human exposure to radio frequency electromagnetic fields, 3 kHz to 300 GHz, 1999.

[5] R.A. Normann, E.M. Maynard, P.J. Rousche, and D.J. Warren, "A neural interface for a cortical vision prosthesis," *Vision Research*, vol. 39, pp. 2577-2587, 1999.

[6] W.H. Ko, S.P. Liang, C.D. Fung, "Design of radio-frequency powered coils for implant instruments," *Med. Biol. Eng. Computing*, vol. 15, pp. 634-640, 1977.

[7] C.M. Zierhofer and E.S. Hochmair, "Geometric approach for coupling enhancement of magnetically coupled coils", *IEEE Trans. Biomed. Eng.*, vol. 43 , no. 7, pp. 708 – 714, July 1996.

[8] D. G. Galbraith, M. Soma, and R. L. White, "A wide-band efficient inductive transdermal power and data link with coupling insensitive gain," *IEEE Trans. Biomed. Eng.*, vol. 34, pp. 265–275, Apr. 1987.

[9] S. Atluri and M. Ghovanloo, "Design of a wideband power-efficient inductive wireless link for implantable biomedical devices using multiple carriers," *Proc. 2nd Intl. IEEE/EMBS Conf. on Neural Engineering*, pp. 533-537, Mar. 2005.

[10] M. Ghovanloo and K. Najafi, "A Wideband Frequency-Shift Keying Wireless Link for Inductively Powered Biomedical Implants", *IEEE Trans. Circ. Sys.* I, vol. 51, no. 12, Dec. 2004.

[11] W. Liu et al., "Implantable biomimetic microelectronic system design," *IEEE Eng. Med. Biol. Mag.*, vol. 24, pp. 66-74, Oct. 2005.

[12] F.W. Grover, "Inductance calculations, working formulas and tables," D. Van Nostrand Co. Inc., New York, 1946.

[13] FastHenry2 available at: http://www.fastfieldsolvers.com/

[14] G.A. Kendir *et al.*, "An optimal design methodology for inductive power link with class-E amplifier, " *IEEE Trans Circuits and Systems I*, vol. 52, pp. 857-866, May 2005.